Dalton Transactions

Aluminium-catalysed intramolecular hydroamination of aminoalkenes: Computational perusal of alternative pathways for aminoalkene activation

Journal:	*Dalton Transactions*
Manuscript ID:	DT-ART-01-2015-000121.R2
Article Type:	Paper
Date Submitted by the Author:	25-Feb-2015
Complete List of Authors:	Tobisch, Sven; University of St. Andrews, School of Chemistry

Cite this: DOI: 10.1039/c0xx00000x

www.rsc.org/xxxxxx

PAPER

Aluminium-catalysed intramolecular hydroamination of aminoalkenes: Computational perusal of alternative pathways for aminoalkene activation

Sven Tobisch*

Received (in XXX, XXX) Xth XXXXXXXXX 20XX, Accepted Xth XXXXXXXXX 20XX
DOI: 10.1039/b000000x

A comprehensive computational examination of alternatively plausible mechanistic pathways for the intramolecular hydroamination (HA) of aminoalkenes utilising a recently reported novel phenylene-diamine aluminium amido compound is presented. On the one hand, a proton-assisted concerted N–C/C–H bond-forming pathway to afford the cycloamine in a single step can be invoked, and, on the other, a stepwise σ-insertive pathway that involves a relatively fast, reversible migratory olefin 1,2-insertion step linked to a less rapid, irreversible Al–C alkyl bond protonolysis. The present study, which employs a sophisticated and reliable computational methodology, supports the prevailing mechanism to be a stepwise σ-insertive pathway. The predicted effective barrier for turnover-limiting aminolysis compares favourably with reported catalytic performance data. Non-competitive kinetic demands militates against the operation of the concerted proton-assisted pathway, which describes N–C bond-forming ring closure triggered by concomitant amino proton delivery at the C=C linkage evolving through a six-centre transition state structure. The valuable insights into mechanistic intricacies of aluminium-mediated intramolecular HA reported herein will help guide the rational design of group 13 metal-based HA catalysts.

Introduction

The catalytic hydroamination (HA) reaction, the direct addition of an N–H bond across an unsaturated carbon–carbon linkage, offers facile access to an industrially relevant organonitrogen commodity and fine chemicals in a waste-free, highly atom-efficient and green manner.[1] The intramolecular HA constitutes a particularly powerful and concise route to functionalised nitrogen heterocycles. Initially dominated by the discovery of organolanthanide catalysts,[1k,2] intramolecular HA research activities are wide ranging over the last two decades, covering the entire periodic table, from early d-block metals,[3-5] 4f-block elements[2] and 5f-block elements[6] to late d-block metals[7,8] and coinage metals.[7b,7n,9]

Research efforts aimed at the development of main-group metal-based catalyst systems have become intensified only in recent years, among them are alkali-,[10] alkaline earth-[11] and group 13 metal[12]-based catalysts. Although abundant and exceedingly inexpensive, aluminium has remarkably little precedent in HA catalysis.[13] Phenylene-diamine (pda) ligated aluminium compounds have been recently reported to competently mediate the cyclisation of aminoalkenes with moderate rates.[12a] The similarity to early d-block metals leads one to reasonably assume that the aluminium-mediated cyclohydroamination shares mechanistic similarities with early transition metal-based systems. Scheme 1 displays principal features of the most plausible among the several mechanistic proposals. The starting material needs to undergo an initial transformation into the catalytically competent metal amidoalkene compound **3**. Thereafter, the HA process is traditionally thought to proceed in a stepwise fashion involving first the insertion of an unsaturated C–C linkage into the metal–N amido σ-bond (**3'**•S → **4**•S) and protonolytic cleavage of the metal–C σ-bond at the metal alkyl intermediate (**4**•S → **5**) thereafter. It is commonly believed for this σ-insertive mechanism (Scheme 1, cycle A) that insertive cyclisation is slow, with M–C σ-bond aminolysis assumed to be significantly faster. However, the observation of a substantial primary kinetic isotope effect (KIE)[2b,3k,3p,4y,4aa,4ab,4ac] and isotopic perturbation of stereoselectivity[2b,3p,4ab] in various catalyst systems is indicative of significant N–H bond disruption in the transition state (TS) structure of the stereo-determining and turnover-limiting N–C bond-formation step. This lead to a proposed alternative proton-assisted pathway that evolves through a multicentre TS structure constituting concerted N–C/C–H bond formation proceeding outside of the metal's immediate vicinity.[2b,6c,14] Commencing from the (pda)Al amidoalkene substrate adduct (**3'**•S), the cycloamine is delivered in a single step via the proton-assisted pathway (Scheme 1, cycle B), thus contrasting the σ-insertive pathway.

The proton-triggered concerted N–C/C–H bond-forming mechanism received increased attention in recent years and was thus suggested for HA of aminoalkenes by some alkaline-earth,[11f,11h,11k] rare earth,[3p] and group 4[4y,4aa,4ab] catalyst systems.

Recent computational studies described the concerted mechanism as a viable but energetically non-competitive alternative in the presence of an operative σ-insertive mechanism tris(oxazolinyl)-borate magnesium alkyl[15a] and also cyclopentadienyl-bis-(oxazolinyl)borate yttrium alkyl[15b] compounds. However, further complementary experimental[4aa] and computational[15c] mechanistic studies have provided compelling evidence for the operation of a proton-assisted concerted mechanism for aminoalkene HA by a bis(ureate) zirconium catalyst.

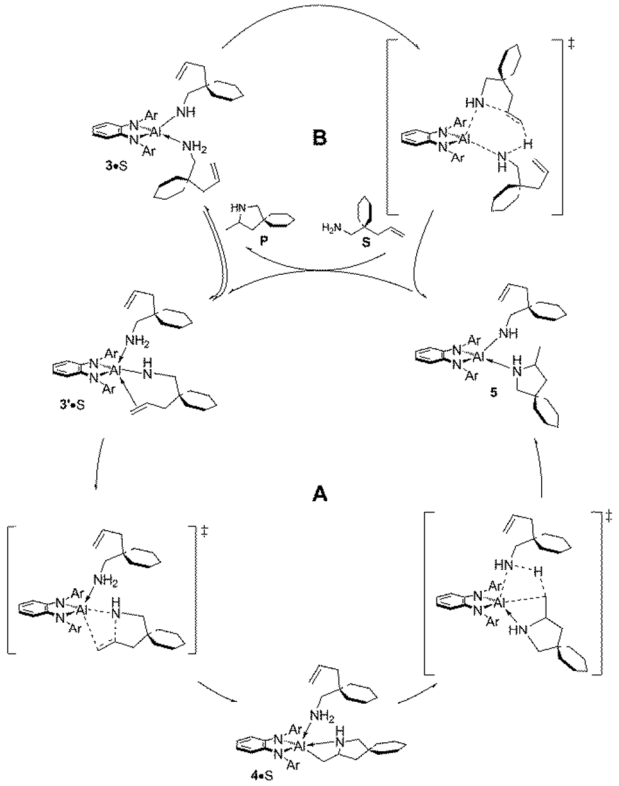

Scheme 1 Plausible mechanistic pathways for phenylene-diamine aluminium-catalysed intramolecular hydroamination, exemplified for [(pda)Al(NHR)•(NH_2R)] aluminium amido **3'**•S as the catalytically competent compound and prototype (1-allylcyclohexyl)-methanamine substrate (S ≡ **1**) ($(pda)^{2-}$ = $[ArN(C_6H_4)NAr]^{2-}$ with Ar = 3,5-^{t}Bu-C_6H_3).

Precise knowledge of both the operative mechanism and of catalytic structure-productivity relationships are required for the rational design of improved HA catalysts. Given that precise details of mechanistic intricacies of aluminium-mediated aminoalkene HA remain largely elusive thus far,[12] we have employed density functional theory (DFT) calculations as an established and predictive means to study reaction mechanism and to guide rational catalyst design. The present study scrutinises competing mechanistic pathways for intramolecular hydroamination of a prototype substrate (1-allylcyclohexyl)-methanamine (S ≡ **1**) by a recently reported[12a] competent phenylene-diamine aluminium amido compound [(pda)Al(NMe_2)•($NHMe_2$)] **2** (where $(pda)^{2-}$ = $[ArN(C_6H_4)NAr]^{2-}$ and Ar = 3,5-^{t}Bu-C_6H_3). No structural simplifications of any kind have been imposed for any of the key species involved.

The DFT methodology employed (dispersion-corrected double-hybrid B2PLYP-D3 in conjunction with basis sets of triple-ζ quality and a sound treatment of bulk solvent effects) simulated authentic reaction conditions adequately and mechanistic analysis is based on Gibbs free-energy profiles. The chosen computational protocol can confidently be expected to reliably map the energy landscape and this has allowed mechanistic conclusions with substantial predictive value to be drawn.

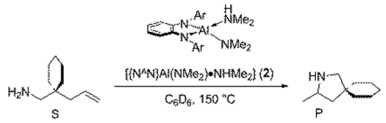

Scheme 2 Intramolecular HA of a primary 2,2-disubstituted aminoalkene by a phenylene-diamine [(pda)Al(NMe_2)•($NHMe_2$)] aluminium amido compound **2** ($(pda)^{2-}$ = $[ArN(C_6H_4)NAr]^{2-}$ with Ar = 3,5-^{t}Bu-C_6H_3).

The comprehensive mechanistic examination presented herein favours a stepwise σ-insertive pathway that entails reversible insertive N–C bond-forming ring closure, linked to slower and irreversible intramolecular Al–C tether σ-bond aminolysis at the transient (pda)Al alkyl intermediate. The assessed barrier for turnover-limiting aminolysis compares well with reported productivity data. On the other hand, an energetically more demanding kinetic profile militates against the operation of a concerted proton-assisted pathway, proceeding through a multi-centre TS structure for the catalyst at hand.

Results and discussion

This study scrutinises all the relevant elementary steps of alternative mechanistic pathways in Scheme 1, with special attention devoted to assess the aptitude for substrate association

for each individual species. It starts with an examination of the transformation of aluminium amido starting material **2** into the catalytically competent (pda)Al amidoalkene compound.

Catalyst initiation

Effective HA catalysis entails the initial transformation of the amine adducted [(pda)Al(NMe$_2$)•(NHMe$_2$)] aluminium amido starting material **2**•A into the catalytically active [(pda)Al(NHR)] aluminium amidoalkene compound. The ability of **2** to effect protonolytic Al–N amido σ-bond cleavage, although being unlikely turnover-limiting, will influence the performance of HA catalysis, because it determines the amount of catalytically competent (pda)Al amidoalkene species available for catalytic turnover.

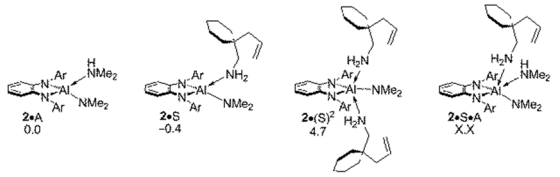

Fig. 1 Amine exchange at the phenylene-diamine aluminium amido starting material **2**.[16,17a]

Dimethylamine (A) and aminoalkene (S) bind equally strongly at aluminium in **2**. The somewhat encumbering phenylene-diamine (pda)Al ligation supports the accommodation of another substrate molecule at aluminium, but at some energy cost, whilst association of a third amine molecule is seen to not be achievable (Fig. 2). On the other hand, **2** exhibits no propensity toward dimer formation as **2**•A is favoured relative to **2ad** (Fig. 1). After the initial facile displacement of HNMe$_2$ by S, the protonolytic cleavage of the Al–N amido σ-bond at substrate adducts **2**•S, **2**•(S)^2 evolves through a metathesis-type TS structure, which decays thereafter into substrate-free and substrate-adducted forms of the aluminium amidoalkene catalyst complex through facile liberation of HNMe$_2$. Figure 2 reveals that pathways with one (via TS[**2**•S–**3**•A]) or two substrate (via TS[**2**•(S)^2–**3**•S•A]) molecules involved appear equally viable kinetically and are identical in thermodynamic terms, because both pathways lead eventually to **3'**•S either by facile amine exchange at **3**•A or by facile amine displacement at **3**•S•A.

Given its affordable kinetic barrier, catalyst initiation through protonolytic Al–N amido σ-bond cleavage should be reasonably rapid at elevated temperatures and is furthermore driven by a small thermodynamic force of 1.1 kcal mol^{-1}. Hence, the transaminative equilibrium between **2** and the catalytically relevant (pda)Al amidoalkene compound favours both sides to a similar extent.

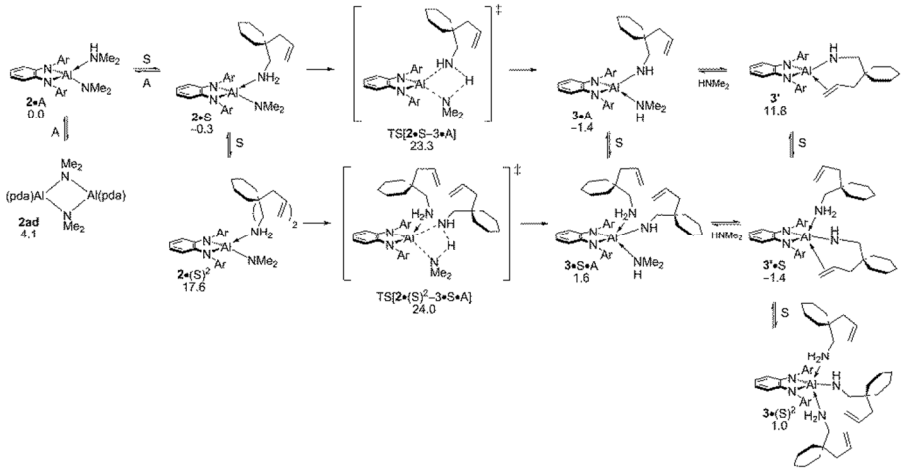

Fig. 2 Al–N amido σ-bond aminolysis at **2** by aminoalkene substrate (S ≡ **1**).[16,17a]

The [(pda)Al(NHR)] compound

Amine substrate (S), cycloamine product (P) together with HNMe$_2$ (A) compete for association onto the catalytically competent [(pda)Al(NHR)] compound and likely gives rise to a multitude of adduct species, all of which are expected to participate in rapid association/dissociation equilibria.[16] Figure 3 summarises the relative stabilities of various located species with one or two adducted amine molecules.[16c] A somewhat sterically encumbering (pda)Al ligation renders amine association at aluminium affordable energetically and favours mono-amine adducted species, like **3**•S or **3**•P, over analogues with two adducted amine molecules, like **3**•(S)^2 or **3**•S•P, and over substrate-free species, like **3**, in particular. The rather large thermodynamic gap for substrate-free species is indicative of some unsaturation around the Al centre in these species. Primary (S) and secondary (P) amines display a propensity of comparable magnitude for binding at aluminium for mono-amine (*cf.* **3**•S and **3**•P) and also for bis-amine (*cf.* **3**•(S)^2 and **3**•S•P) adducts.

With the focus on catalytically relevant [(pda)Al(NHR)•(S)^n] species the pattern of amidoalkene complexation for substrate-free and substrate-adducted species largely reflects the varying spatial demands around the Al centre. For substrate-free forms, species **3'** featuring an amidoolefin unit that forms a weak chelate by orienting its double bond proximal to aluminium (thereby compensating for a degree of unsaturation within the coordination sphere around the Al centre) is thermodynamically favoured over **3** with a monohapto *N*-ligated amidoolefin unit. The gap becomes significantly narrowed for mono-amine adducted species, with **3'**•S is now preferred over **3**•S only marginally, whilst the order

of relative stability becomes inverted for bis-amine adducts. Due to a further saturation of the coordination sphere around aluminium by a second associated substrate molecule, the tendency to accommodate a chelating amidoalkene unit rapidly deteriorates. Despite some efforts an energetically approachable **3'**•$(S)^2$ species could not be located, hence **3**•$(S)^2$ prevails energetically for bis-amine adducts.

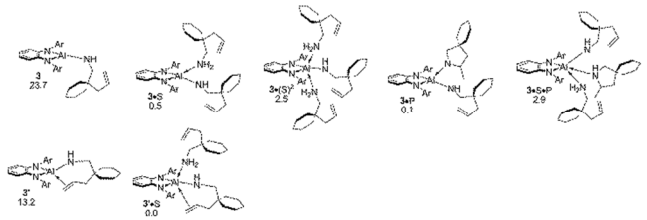

Fig. 3 Amine association at the catalytically competent [(pda)Al(NHR)] compound.[16,17b]

Overall DFT reveals that primary (S) and secondary (P) amines bind in comparable strength at the catalytically competent [(pda)Al(NHR)] compound. It does predominantly exist as mono-substrate adducted species (**3'**•S and **3**•S), together with a less populated bis-substrate adduct **3**•$(S)^2$.

The σ-insertive mechanism

The analysis of proposed alternative mechanistic scenarios starts with an examination of the σ-insertive mechanism (Scheme 1, cycle A) that involves: migratory olefin 1,2-insertion into the Al–N amido σ-bond to proceed at **3'** or its substrate adducted analogues; followed by intramolecular protonolytic cleavage of the Al–C azacycle tether σ-bond at the (pda)Al alkyl intermediate by an aluminium bound substrate molecule. In light of the pronounced aptitude of the (pda)Al amido to favourably bind additional amine molecules, it can reasonably be anticipated that viable pathways for insertive cyclisation may see the participation of bound amine serving as a spectator, but effects intramolecular Al–C bond aminolysis thereafter.

Migratory olefin 1,2-insertion into the Al–C amido σ-bond. Several imaginable trajectories for insertive cyclisation that starts from **3'** or its mono-substrate adduct **3'**•S have been examined. Figure 4 collates the condensed energy profiles for **3**•$(S)^n$ → **4**•$(S)^n$ (n = 0, 1) insertive cyclisation proceeding through the most accessible pathways; the full account of all the studied pathways can be found in the SI package (Figs. S1–S3 in the ESI†). Common to all the trajectories examined is that N–C bond-forming ring closure evolves through a planar four-centre TS structure describing metal-mediated olefin 1,2-insertion into the Al–C amido σ-bond that occurs at distances of approximately 2.0 Å for the emerging N–C bond (Fig. S1 in the ESI†). Following the reaction path further, TS structures decay into the (pda)Al alkyl intermediate **4**•$(S)^n$, which has the azacycle bound to aluminium through its methylene tether and the nitrogen donor centre.

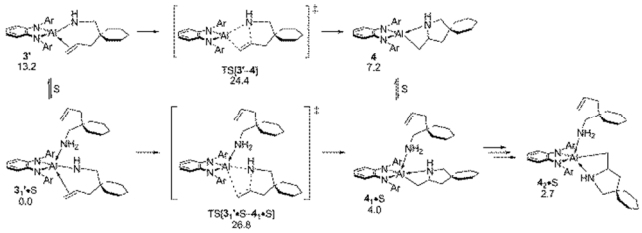

Fig. 4 Most accessible pathways for migratory olefin insertion into the Al–N amido σ-bond at **3'** and its substrate adducted species **3'**•S.[16,17b]

Insertive cyclisation via pathways with one substrate molecule participating preferably proceeds commencing from the prevalent (pda)Al(NHR) species $\mathbf{3_1}$'•S through a trajectory featuring an axial olefin approach, whilst the alternative trajectory for equatorial olefin approach is found somewhat less favourable kinetically (Fig. S3 in the ESI†). The $\mathbf{3_1}$'•S → $\mathbf{4_1}$•S cyclisation has a barrier of 26.8 kcal mol^{-1} to overcome and sees the facile conversion[16b] of the initially formed (pda)Al alkyl $\mathbf{4_1}$•S into the more stable $\mathbf{4_2}$•S isomer that features an azacycle ligation through its equatorial methylene tether and axial N centre. Because the newly established azacycle aluminium coordination cannot completely compensate for the cleavage of the Al–N(amido) bond, it places $\mathbf{4_2}$•S 2.7 kcal mol^{-1} above $\mathbf{3_1}$'•S in free energy. Although a single adducted substrate molecule greatly stabilises the (pda)Al(NHR) compound (*cf.* the thermodynamic gap between **3'** and **3'**•S in Fig. 3) an olefin unit that approaches aluminium more closely in TS[**3'**–**4**] appears to alleviate the degree of coordinative unsaturation around the Al centre due to the absence of associated amine molecules. DFT predicts that insertive cyclisation benefits from temporary amine dissociation kinetically, but not thermodynamically. As revealed from Fig. 4, TS[**3'**–**4**] prevails energetically over TS[$\mathbf{3_1}$'•S–$\mathbf{4_1}$•S], whilst both substrate-free **3'** and **4** are stabilised by coordination of a single amine molecule. On the other hand, two adducted amine spectator molecules are likely of limiting the accessibility of the aluminium by the double bond for a spatially encumbering (pda)Al catalyst backbone. All the efforts of locating energetically approachable precursor or TS structures that participate via **3'**•$(S)^2$ → **4**•$(S)^2$ insertive cyclisation have been unsuccessful. Hence, a sufficiently effective activation of the olefin unit towards a nucleophilic amido approach through its close interaction with the electropositive aluminium can only be maintained for pathways with a maximum of one spectator substrate molecule participating.

Migratory insertion into the polar Al–N amido σ-bond benefits thermodynamically from the participation of one adducted spectator substrate molecule, whilst a planar four-centre TS structure, which has no additional amine molecule coordinated, is preferably traversed. The most accessible pathway commences from the prevalent (pda)Al(NHR) species $\mathbf{3_1}$'•S, which sees an initial dissociation of S prior to N–C bond formation evolving through TS[**3'**–**4**] and a rapid re-association of S at the (pda)Al alkyl intermediate.[16a] This pathway has a barrier of 24.4 kcal mol^{-1} (relative to $\mathbf{3_1}$'•S) to overcome and is somewhat endergonic. It characterises insertive ring closure for a (pda)Al amidoalkene catalyst complex as a kinetically viable, reversible transformation that favours the reactant.

Al–C azacycle tether bond aminolysis. The (pda)Al alkyl species that is generated via the most accessible pathway for insertive cyclisation already has a substrate molecule bound at aluminium that is moreover favourably placed *cis* to the equatorial Al–C tether linkage. Notwithstanding of this fortunate arrangement, several conceivable trajectories for intramolecular H transfer have been examined that may benefit from the participation of additional amine molecules (*cf.* Figs. S4–S6 in the ESI†).

Aminolysis evolves through a metathesis-type TS structure that describes the cleavage of an already suitably polarised N–H bond and concomitant C–H bond formation. The process to commence at **4**•S and **4**•$(S)^2$ favourably proceeds through a trajectory that constitutes the cleavage of an equatorial aluminium alkyl bond by a proton released from an axial metal bound, hence acidified substrate molecule (Fig. 5). The association of an amine spectator molecule at **4**•S is favoured in terms of enthalpy, but its magnitude is not large enough to compensate for the associated entropy penalty. It places pathways with two substrate molecules participating at a higher energy than pathways with a single molecule involved (Fig. 5). It is noted that the intrinsic barrier (25.7 kcal mol^{-1} for $\mathbf{4}_2$•S → **5**, relative to $\mathbf{4}_2$•S) increases (27.1 kcal mol^{-1} for $\mathbf{4}_2$•$(S)^2$ → $\mathbf{5}_2$•S, relative to $\mathbf{4}_2$•$(S)^2$) as a result of substrate coordination, thereby reflecting the spatial demand imposed by the (pda)Al catalyst backbone. Hence, additionally associated spectator amine molecules are unlikely to facilitate the process on either thermodynamic or kinetic grounds.

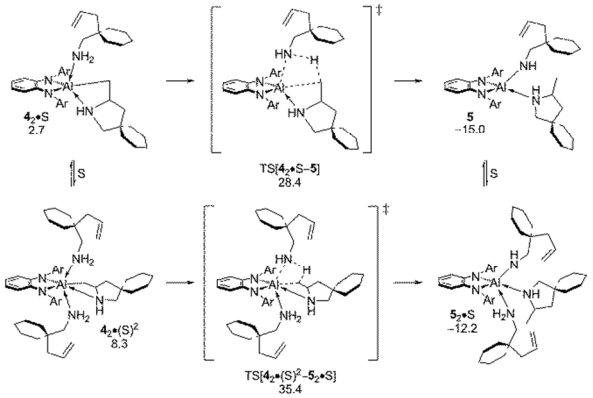

Fig. 5 Most accessible pathways for Al–C σ-bond aminolysis at amine-adducted species **4**•S and **4**•$(S)^2$ of the (pda)Al alkyl intermediate.[16,17b]

The most accessible $\mathbf{4}_2$•S → **5** pathway features a barrier of 25.7 kcal mol^{-1} and affords [(pda)Al(NHR)•(NHRR)] compound **5** in a process that is downhill by 17.7 kcal mol^{-1} (relative to $\mathbf{4}_2$•S). Incoming substrate S readily displaces[16a,b] the pyrrolidine at **5**•S in a thermoneutral transformation (ΔG = –0.1 kcal mol^{-1} for **5**•S + S → $\mathbf{3}_1$'•S + P), thereby completing cycle A in Scheme 1 with the regeneration of the catalytically competent (pda)Al amidoalkene compound for another catalyst turnover.

Generation of the (pda)Al pyrrolide compound. An aluminium pyrrolide **6**•$(S)^n$ has been observed by NMR spectroscopy upon monitoring the stoichiometric reaction of **2** with 2,2-diphenylpent-4-ene-1-amine.[12a] Provided that the pyrrolide is kinetically accessible at affordable cost, it could well compete with [(pda)Al(NHR)•(NH_2R)] $\mathbf{3}_1$'•S and [(pda)Al(NHR)•(NHRR)] **5**•S for constituting the catalyst resting state. Plausible pathways for the generation of (pda)Al pyrrolide **6**•$(S)^n$ have been examined, including: i) cycloamine α-proton abstraction at **5**•$(S)^n$; and: ii) intramolecular 1,3 H-transfer at the Al alkyl **4**•$(S)^n$, a process that may benefit from the participation of additional amine molecules through a relay-type mechanism. The first pathway proves to be energetically far more accessible when compared to the second one and is thus likely the prevailing route that leads to **6**•$(S)^n$. It is noted that a similar conclusion has been drawn for a tris(oxazolinyl)borate magnesium catalyst.[15a]

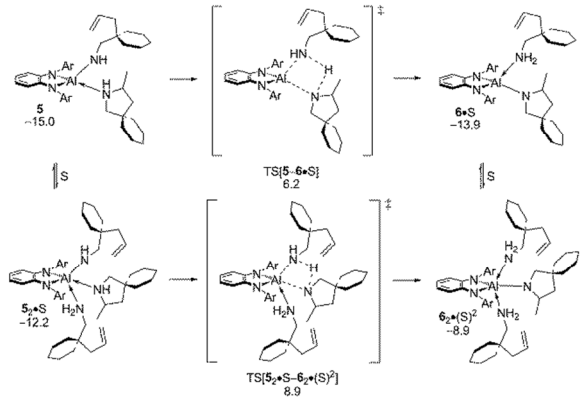

Fig. 6 Most accessible pathways for conversion of the (pda)Al amido cycloamine compound **5** into (pda)Al pyrrolide intermediate **6**.[16,17b]

The condensed energy profiles (Fig 6) of the most accessible pathways to commence from **5** and **5**•S, both of which are formed via the dominant **4**•$(S)^n$ → **5**•$(S)^{n-1}$ (n = 0, 1) pathways for protonolytic Al–C bond cleavage (*cf.* Fig. 5), reveals that α-proton abstraction preferably proceeds at **5**. The process is unlikely facilitated by an adducted amine spectator molecule, hence paralleling the findings for the protonolysis step. Proton transfer evolves through a metathesis-type TS[**5**–**6**•S] with a barrier of 21.2 kcal mol^{-1} to afford substrate-adducted (pda)Al pyrrolide **6**•S, which is 1.1 kcal mol^{-1} higher in free energy. Hence, **5** ⇄ **6**•S pyrrolidine → pyrrolide conversion describes a kinetically viable equilibrium that somewhat favours [(pda)Al(NHR) •(NHRR)] intermediate **5**. The mono-substrate adduct **6**•S is the prevalent form of the (pda)Al pyrrolide compound with bis-substrate adducted $\mathbf{6}_2$•$(S)^2$ and substrate-free **6** species are at higher energy, separated by 5.0 and 20.2 kcal mol^{-1} (relative to **6**•S), respectively.

The concerted proton-triggered cyclisation mechanism

The alternative mechanistic pathway B outlined in Scheme 1, which describes N–C ring closure triggered by concomitant amino proton transfer onto the adjacent C=C linkage, thereby affording cycloamine products through a concerted single-step transformation, is examined next. For the process to be assisted by an adducted spectator substrate molecule, the two examined trajectories involving N–C bond formation through an axial olefin approach at the Al–N amido σ-bond, triggered by a proton transferred from an equatorially bound substrate, or alternatively describing concurrent ring closure through equatorial olefin approach and proton delivery from an axially bound substrate, are found to be almost indistinguishable kinetically, with the

trajectory for equatorial olefin approach marginally favoured (*cf.* Fig. S12 in the ESI†). The concerted amidoalkene → cycloamine conversion proceeding through the most accessible **3**•S → **5** and **3**•$(S)^2$ → $\mathbf{5}_2$•S pathways (Fig. 7) evolve through a six-centre TS structure that constitutes N–C^5 ring closure with concomitant transfer of an aluminium bound, hence acidified substrate molecule at the adjacent olefin–C^6 centre. As exemplified in Fig. 8 for the **3**•S → **5** pathway, the located TS[**3**•S–**5**] structure occurs at a N–C^5 distance of 2.05 Å and features emerging C–H (1.47 Å) and vanishing N–H (1.27 Å) bonds, all of which is indicative of a concerted, but asynchronous proton transfer. The rather distinct spatial separation of the C=C linkage apart from aluminium (Al–olefin distance >3.5 Å) describes N–C ring closure taking place outside of the immediate vicinity of the metal, thereby reflecting that amino proton delivery activates the double bond towards nucleophilic amido approach and not close interaction with the electropositive Al centre as necessitated in cycle A. After passing through the TS structure, TS[**3**•S–**5**] and TS[**3**•$(S)^2$–$\mathbf{5}_2$•S] decay into the (pda)Al amido pyrrolidine compound **5** and its substrate adduct $\mathbf{5}_2$•S, respectively.

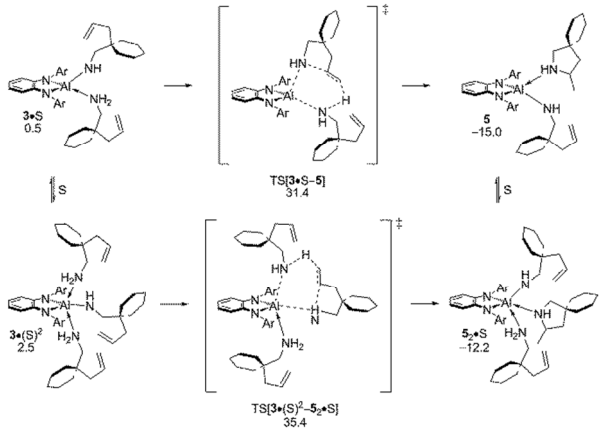

Fig. 7 Most accessible pathways for N–C bond formation with concurrent delivery of the amino proton to the olefin unit at the [(pda)Al(NHR)] compound with one (**3**•S, top) or two (**3**•$(S)^2$, bottom) adducted substrate molecules.[16,17b]

The concurrent N–C ring closure and amino proton delivery to commence at **3**•S and evolving through a multi-centre TS structure describes the energetically prevalent pathway for the single-step amidoalkene → cycloamine transformation. It has a barrier of 30.9 kcal mol^{-1} to overcome and affords [(pda)Al(NHR)•(NHRR)] compound **5** in a process that is downhill by 14.5 kcal mol^{-1} (Fig. 7, relative to **3**•S). Thus, proton-assisted concerted N–C/C–H bond formation is irreversible as is Al–C alkyl bond aminolysis and both steps furnish **5**. Similar to previous discussion for insertive cyclisation and aminolysis steps, the association of another spectator amine molecule does not serve stabilising either of reactant, product of TS structures and additional amine molecules are therefore unlikely to participate in this step (Fig. 7). It is worth mentioning that the kinetic gap between pathways with and without an adducted amine spectator molecule participating narrows from 7.0 kcal mol^{-1} for protonolysis (Fig. 5) to 4.1 kcal mol^{-1} (Fig. 7) for concerted proton-triggered cyclisation, whilst, on the other hand, limitations in the accessibility of the Al centre due to amine association makes **3'**•$(S)^2$ → **4**•$(S)^2$ insertive cyclisation impossible to achieve. This behaviour reflects the difference in spatial demands imposed by the phenylene-diamine ligand on the aluminium centre whilst traversing σ-insertive and concerted proton-triggered mechanistic pathways, with the latter being least susceptible to steric pressure.

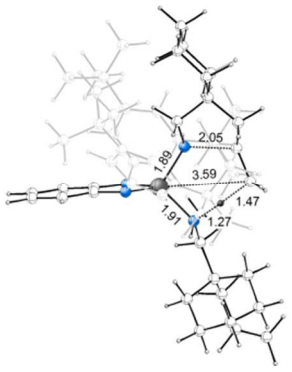

Fig. 8 Selected structural parameter (angstroms) of the located TS structure for proton-assisted concerted N–C/C–H bond formation at **3**•S.[18]

Comparison of mechanistic pathways

Having completed the examination of relevant elementary steps for alternative cycles A and B in Scheme 1, Fig. 9 collates the assessed free-energy profiles of the two mechanistic scenarios for cyclohydroamination of aminoalkene S to be mediated by phenylene-diamine (pda)Al amido starting material **2**. It focuses exclusively on the most accessible pathways to commence from the catalytically competent phenylene-diamine [(pda)Al(NHR)•(NH_2R)] amidoalkene compound, which is readily generated through initial catalyst activation, whereas other less probable or energetically prohibitive pathways have been omitted.

With regard to the identity of the catalyst resting state, (pda)Al amidoalkene **3'**•S and (pda)Al amido cycloamine **5** (≡ **3**•P) are found almost indistinguishable energetically (Fig. 3), whilst the third conceivable candidate, that is (pda)Al pyrrolide **6**•S is found slightly less favourable (Fig. 6). In light of the predicted narrow energy gap of 1.1 kcal mol^{-1} between these three candidates, it would be imprudent speculating on the precise nature of the catalyst resting state.

The N–C bond-forming ring closure with concurrent amino proton transfer taking place outside of the immediate proximity of the electropositive aluminium centre through a six-centre TS[**3**•S–5] structure is irreversible and has a barrier of 31.4 kcal mol^{-1} (relative to $\mathbf{3}_1$'•S)[19] to overcome. The σ-insertive mechanistic pathway entails 1) relatively fast, reversible σ-insertive N–C bond-forming cyclisation ($\Delta G^{\ddagger}$ = 24.4 kcal mol^{-1}, relative to $\mathbf{3}_1$'•S)[19] that favours the Al amidoalkene catalyst species and benefits kinetically from a temporary dissociation of adducted S; 2) slow and downhill protonolytic Al–C σ-bond cleavage at the (pda)Al alkyl intermediate ($\Delta G^{\ddagger}$ = 28.4 kcal mol^{-1}, relative to $\mathbf{3}_1$'•S)[19]; followed by 3) kinetically easy displacement of cycloamine by substrate to regenerate the (pda)Al amidoalkene active catalyst complex.

It is noteworthy that the two mechanistic cycles are driven by a thermodynamic force of identical magnitude and are indistinguishable by an empirical rate law (provided that the catalyst species is identical) or by the observation of a substantial

primary KIE. DFT reveals that a proton-assisted concerted N–C/C–H bond-forming pathway is energetically prohibitive in the presence of a kinetically less demanding σ-insertive pathway. The magnitude of the kinetic disparity ($\Delta\Delta G^{\ddagger}$ = 3.0 kcal mol^{-1}, Fig. 9) assessed by application of a high-level computational protocol is indicative that the σ-insertive pathway is likely traversed exclusively. The DFT predicted total barrier of 28.4 kcal mol^{-1} (relative to $\mathbf{3_1}$'•S)[19] for turnover-limiting aluminium alkyl bond aminolysis compares favourably with reported data on catalytic performance.[12a,20]

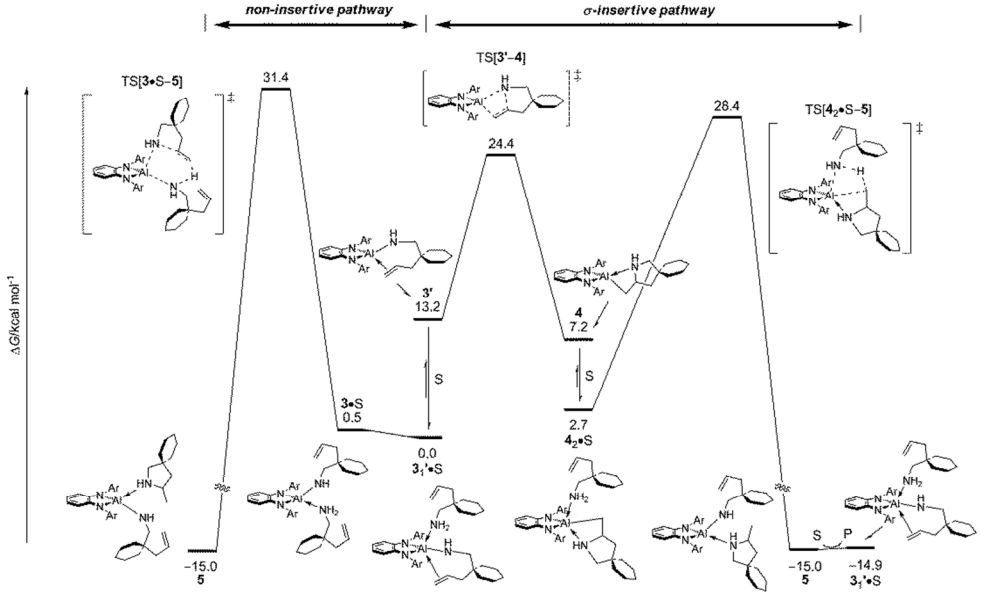

Fig. 9 Condensed reaction profile for intramolecular hydroamination of aminoalkene S by an phenylene-diamine (pda)Al amido catalyst proceeding through alternative mechanistic cycles. Pyrrolidine product liberation through **5** + S → $\mathbf{3_1}$'•S + P is included ((pda)$^{2-}$ = [ArN(C_6H_4)NAr]$^{2-}$ with Ar = 3,5-^{t}Bu-C_6H_3).

Conclusion

With the aim to develop the mechanistic insight into the group 13 metal-mediated intramolecular hydroamination of aminoalkenes, DFT as an established and predictive method has been employed to scrutinise plausible mechanistic scenarios for cyclisation of prototype (1-allylcyclohexyl)-methanamine **1** by a recently reported[12a] novel phenylene-diamine [(pda)Al(NMe_2)•($NHMe_2$)] aluminium amido compound **2** ((pda)$^{2-}$ = [ArN(C_6H_4)NAr]$^{2-}$ with Ar = 3,5-^{t}Bu-C_6H_3). Firstly, a proton-triggered concerted N–C/C–H bond-forming mechanism, thereby accomplishing amidoalkene → cycloamine transformation in a single step and secondly, a stepwise σ-insertive pathway that involves relatively fast and reversible migratory olefin 1,2-insertion into to Al–N amido σ-bond linked to irreversible and slower Al–C alkyl bond aminolysis. The detailed computational examination presented herein discloses non-competitive kinetic demands for a pathway describing N–C bond-forming ring closure taking place outside of the immediate proximity of the electropositive aluminium centre provoked by concurrent amino proton delivery at the C=C linkage evolving through a six-centre TS structure. It militates against the operation of a concerted non-insertive cyclisation pathway in the presence of a kinetically favourable σ-insertive pathway. This pathway involves 1) relatively fast, reversible σ-insertive N–C bond-forming cyclisation that benefits kinetically from a temporary dissociation of adducted S and favours the Al amidoalkene catalyst species; 2) turnover-limiting downhill protonolytic Al–C σ-bond cleavage at the (pda)Al alkyl intermediate; followed by 3) kinetically easy displacement of cycloamine by substrate to regenerate the (pda)Al amidoalkene active catalyst complex. The magnitude of the assessed kinetic disparity indicates that the σ-insertive pathway is likely traversed exclusively. The DFT predicted effective barrier for turnover-limiting aluminium alkyl bond aminolysis compares favourably with reported catalytic performance data.[12a,20]

Computational Methodology

All calculations based on Kohn-Sham density functional theory (DFT)[21] were performed by means of the program package TURBOMOLE[22] employing flexible basis sets of triple-ζ quality. The Becke-Perdew (BP86)[23] generalized gradient approximation (GGA) functional within the RI-*J* integral approximation[24] in conjunction with appropriate auxiliary basis sets was used for structure optimisation. Empirical dispersion corrections by Grimme (D3 with Becke-Johnson damping)[25] were used to account for critical non-covalent interactions involved in the studied HA catalysis. Aluminium was treated by the (14s9p3d1f)/[5s5p3d1f] (def2-TZVPP) all-electron basis set,[26] whilst all remaining elements were represented by Ahlrich's valence triple-ζ TZVP basis set[27a,b] with polarization functions on all atoms. Final potential energies were obtained by single point calculations at BP86 optimised structures using the double-hybrid B2PLYP[28] functional (together with D3(BJ) empirical dispersion correction)[25] in conjunction with a def2-TZVPP basis set for aluminium and a def2-TZVP basis set[26] for all remaining elements (B2PLYP-D3(def2-TZVPP + def2-TZVP)//BP86-D3 (def2-TZVPP + def-TZVP)).

The reaction pathways were explored by a chain-of-states method,[29] as implemented in the module *woelfling* in the TURBOMOLE suite of programs, which makes use of reasonably chosen reactant and product structures to deliver an approximate to the minimum energy path (MEP). It identified the reactant and product states to be linked to the associated transition state. The approximate saddle points connected with the MEP were subjected to an exact localisation of the TS structures. The geometry optimisation and the saddle-point search were carried out by utilising analytical/numerical gradients/Hessians according to standard algorithms. No symmetry constraints were imposed in any case. The stationary points were identified exactly by the curvature of the potential energy surface at these points corresponding to the eigenvalues of the Hessian. All reported transition states possess exactly one negative Hessian eigenvalue, while all other stationary points exhibit exclusively positive eigenvalues.

The free-energy landscape of the entire HA course was assessed for (1-allylcyclohexyl)-methanamine substrate (S ≡ **1**) together with an phenylene-diamine [(pda)Al(NHR)•(NH_2R)$_n$] aluminium amidoalkene as catalytically relevant compound. No structural simplification of any of the key species involved was imposed. The DFT calculations have simulated the authentic reaction conditions by treating the bulk effects of the benzene solvent by a consistent continuum model in form of the conductor-like screening model for realistic solvents (COSMO-RS).[30] This solvation model includes continuum electrostatic and also solvent-cavitation and solute-solvent dispersion effects through surface-proportional terms. The free solvation enthalpy has been assessed with the aid of COSMO-RS at the BP86[23]/def2-TZVPD//BP86-D3/def2-TZVPD[26] level of approximation. Frequency calculations were performed for stationary points that were located at the BP86-D3/(def2-TZVPP + SV(P))[27c] level to confirm the nature of all optimised key structures and to determine thermodynamic parameters (423 K, 1 atm) under the conventional ideal-gas, rigid-rotor and quantum-mechanical harmonic-oscillator approximation. The entropy contributions for condensed-phase conditions were estimated based on computed gas-phase entropies by employing the procedure of Okuno.[31] The mechanistic conclusions drawn in this study were based on the Gibbs free-energy profile of the entire catalytic cycle assessed at the B2PLYP-D3(COSMO-RS)/(def2-TZVPP + def2-TZVP) level of approximation for experimental condensed phase conditions. Calculated structures were visualised by employing the StrukEd program,[32] which was also used for the preparation of 3D molecule drawings.

Notes and references

School of Chemistry, University of St Andrews, Purdie Building, North Haugh, St Andrews, United Kingdom KY16 9ST.
E-mail: st40@st-andrews.ac.uk; Fax (+44) 1797-383-652

† Electronic Supplementary Information (ESI) available: Additional details. See DOI: 10.1039/b000000x/

1 For reviews of catalytic hydroamination, see: (a) L. S. Hegedus, *Angew. Chem.*, 1988, **100**, 1147, (*Angew. Chem. Int. Ed. Engl.*, 1998, **27**, 1113); (b) D. M. Roundhill, *Catal. Today*, 1997, **37**, 155; (c) T. E. Müller and M. Beller, *Chem. Rev.*, 1988, **98**, 675; (d) M. Nobis and B. Drießen-Hölscher, *Angew. Chem.* 2001, **113**, 4105, (*Angew. Chem. Int. Ed.*, 2001, **40**, 3983; (e) R. Taube, in *Applied Homogeneous Catalysis with Organometallic Complexes*, ed. B. Cornils and W. A. Herrmann, Wiley-VCH, Weinheim, 2002, pp 513–524; (f) F. Seayad, A. Tillack, C. G. Hartung and M. Beller, *Adv. Synth. Catal.*, 2002, **344**, 795; (g) G. A. Molander and J. A. C. Romero, *Chem. Rev.*, 2002, **102**, 2161; (h) F. Pohlki and S. Doye, *Chem. Soc. Rev.*, 2003, **32**, 104; (i) P. W. Roesky and T. E. Müller, *Angew. Chem.*, 2003, **115**, 2812, (*Angew. Chem. Int. Ed.*, 2003, **42**, 2708); (j) J. F. Hartwig, *Pure Appl. Chem.*, 2004, **76**, 507; (k) S. Hong and T. J. Marks, *Acc. Chem. Res.*, 2004, **37**, 673; (l) K. C. Hultzsch, *Adv. Synth. Catal.*, 2005, **347**, 367; (m) A. L. Odom, *Dalton Trans.*, 2005, 225; (n) R. Severin and S. Doye, *Chem. Soc. Rev.*, 2007, **36**, 1407; (o) I. Aillaud, J. Collin, J. Hannedouche and E. Schulz, *Dalton Trans.*, 2007, 5105; (p) J. F. Hartwig, *Nature*, 2008, **455**, 314; (q) T. E. Müller, K. C. Hultzsch, M. Yus, F. Foubelo and M. Tada, *Chem. Rev.*, 2008, **108**, 3795; (r) S. Doye, in *Science of Synthesis*, Thieme, Stuttgart, **2009**, vol. 40a, pp 241–304; (s) P. S. Hanley and J. F. Hartwig, *Angew. Chem. Int. Ed.*, 2013, **52**, 8510.

2 For cyclohydroamination mediated by organolanthanides, see: (a) M. R. Gagné and T. J. Marks, *J. Am. Chem. Soc.*, 1989, **111**, 4108; (b) M. R. Gagné and T. J. Marks, *J. Am. Chem. Soc.*, 1992, **114**, 275; (c) Y. Li, P.-F. Fu and T. J. Marks, *Organometallics* 1994, **13**, 439; (d) Y. Li and T. J. Marks, *J. Am. Chem. Soc.*, 1996, **118**, 9295; (e) G. A. Molander and E. D. Dowdy, *J. Org. Chem.*, 1998, **63**, 8983; (f) M. R. Bürgstein, H. Berberich and P. W. Roesky, *Organometallics*, 1998, **17**, 1452; (g) V. M. Arredondo, F. E. McDonald and T. J. Marks, *Organometallics*, 1999, **18**, 1949; (h) A. T. Gilbert, B. L. Davis, T. J. Emge and R. D. Broene, *Organometallics*, 1999, **18**, 2125; (i) G. A. Molander and E. D. Dowdy, *J. Org. Chem.*, 1999, **64**, 6515; (j) Y. K. Kim, T. Livinghouse and J. E. Bercaw, *Tetrahedron Lett.*, 2001, **42**, 2944; (k) G. A. Molander, E. D. Dowdy and S. K. Pack, *J. Org. Chem.*, 2001, **66**, 4344; (l) M. R. Bürgstein, H. Berbericha and P. W. Roesky, *Chem. Eur. J.*, 2001, **7**, 7078; (m) S. Hong and T. J. Marks, *J. Am. Chem. Soc.*, 2002, **124**, 7886; (n) S. Hong, S. Tian, M. V. Metz and T. J. Marks, *J. Am. Chem. Soc.*, 2003, **125**, 14768; (o) S. Hong, A. M. Kawaoka and T. J. Marks, *J. Am. Chem. Soc.*, 2003, **125**, 15878; (p) A. Zulys, T. K. Panda, M. T. Gamer and P. W. Roesky, *Chem. Commun.*, 2004, 2584; (q) J.-S. Ryu, T. J. Marks and F. E. McDonald, *J. Org. Chem.*, 2004, **69**, 1028; (r) A. M. Seyam, B. D. Stubbert, T. R. Jensen, J. J. O'Donnell, III, C. L. Stern and T. J. Marks, *Inorg. Chim. Acta*, 2004, **357**, 4029; (s) J. Collin, J.-C. Daran, O. Jacquet, E. Schulz and A. Trifonov, *Chem. Eur. J.*, 2005, **11**, 3455.

3 For cyclohydroamination mediated by rare earth metals, see: (a) Y. K. Kim and T. Livinghouse, *Angew. Chem.*, 2002, **114**, 3797, (*Angew. Chem. Int. Ed.*, 2002, **41**, 3645); (b) Y. K. Kim, T. Livinghouse and Y. Horino, *J. Am. Chem. Soc.*, 2003, **125**, 9560; (c) P. N. O'Shaughnessy, P. D. Knight, C. Morton, K. M. Gillespie and P. Scott, *Chem. Commun.*, 2003, **14**, 1770; (d) D. V. Gribkov, K. C. Hultzsch and F. Hampel, *Chem. Eur. J.*, 2003, **9**, 4796; (e) J. Collin, J.-C. Duran, E. Schulz and A. Trifonov, *Chem. Commun.*, 2003, 3048; (f) F. Lauterwasser, P. G. Hayes, St. Bräse, W. E. Piers and L. L. Schafer, *Organometallics*, 2004, **23**, 2234; (g) D. V. Gribkov and K. C. Hultzsch, *Chem. Commun.*, 2004, 730; (h) K. C. Hultzsch, F. Hampel and Th. Wagner, *Organometallics*, 2004, **23**, 2601; (i) J. Y. Kim and T. Livinghouse, *Org. Lett.*, 2005, **7**, 4391; (j) T. K. Panda, A. Zulys, M. T. Gamer and P. W. Roesky, *Organometallics*, 2005, **24**, 2197; (k) D. V. Gribkov, K. C. Hultzsch and F. Hampel, *J. Am. Chem. Soc.*, 2006, **128**, 3748; (l) S. Bambirra, H. Tsurugi, D. van Leusen and B. Hessen, *Dalton Trans.*, 2006, 1157; (m) S. Datta, M. T. Garner and P. W. Roesky, *Organometallics*, 2008, **27**, 1207; (n) L. J. E. Stanlake and L. L. Schafer, *Organometallics*, 2009, **28**, 3990; (o) N. K. Hangaly; A. R. Petrov; K. A. Rufanov; K. Harms, M. Elfferding and J. Sundermeyer, *Organometallics*, 2011, **30**, 4544; p) K. Manna, M. L. Kruse and A. D. Sadow, *ACS Catalysis*, 2011, **1**, 1637; (q) Y. Chapurina, H. Ibrahim, R. Guillot, E. Kolodziej, J. Collin, A. Trifonov, E. Schulz and J. Hannedouche, *J. Org. Chem.*, 2011, **76**, 10163.

4 For cyclohydroamination mediated by group 4 metals, see: (a) P. L. McGrane and T. Livinghouse, *J. Org. Chem.*, 1992, **57**, 1323; (b) P. L. McGrane, M. Jensen and T. Livinghouse, *J. Am. Chem. Soc.*, 1992, **114**, 5459; (c) P. L. McGrane and T. Livinghouse, *J. Am. Chem. Soc.*, 1993, **115**, 11485; (d) I. Bytschkov and S. Doye,

Tetrahedron Lett., 2002, **43**, 3715; (e) L. Ackermann and R. G. Bergman, *Org. Lett*., 2002, **4**, 1475; (f) L. Ackermann and R. G. Bergman, *J. Am. Chem. Soc*., 2003, **125**, 11956; (g) C. Li, R. K. Thomson, B. Gillon, B. O. Patrick and L. L. Schafer, *Chem. Commun*., 2003, 2462; (h) D. V. Gribkov and K. C. Hultzsch, *Angew. Chem*., 2004, **116**, 5659, (*Angew. Chem. Int. Ed*., 2004, **43**, 5542); (i) P. A. Knight, I. Munslow, P. N. O'Shaughnessy and P. Scott, *Chem. Commun*., 2004, 894; (j) J. A. Bexrud, J. D. Beard, D. C. Leitch and L. L. Schafer, *Org. Lett*., 2005, **7**, 1959; (k) H. Kim, P. H. Lee and T. Livinghouse, *Chem. Commun*. 2005, 5205; (l) J. R. Petersen, J. M. Hoover, W. S. Kassel, A. L. Rheingold and A. R. Johnson, *Inorg. Chim. Acta*, 2005, **358**, 687; (m) A. Heutling, F. Pohlki, I. Bytschkov and S. Doye, *Angew. Chem*., 2005, **117**, 3011, (*Angew. Chem. Int. Ed*., 2005, **44**, 2951); (n) R. K. Thomson, J. A. Bexrud and L. L. Schafer, *Organometallics*, 2006, **25**, 4059; (o) C. Müller, C. Loos, N. Schulenburg and S. Doye, *Eur. J. Org. Chem*., 2006, 2499; (p) D. A. Watson, M. Chiu and R. G. Bergman, *Organometallics*, 2006, **25**, 4731; (q) M. C. Wood, D. C. Leitch, C. S. Yeung, J. A. Kozak and L. L. Schafer, *Angew. Chem*., 2007, **119**, 358, (*Angew. Chem. Int. Ed*., 2007, **46**, 354); (r) L. Ackermann, L. T. Kaspar, and A. Althammer, *Org. Biomol. Chem*., 2007, **5**, 1975; (s) A. L. Gott, A. J. Clarke, G. J. Clarkson and P. Scott, *Chem. Commun*., 2008, 1422; (t) A. L. Majumder and A. L. Odom, *Organometallics*, 2008, **27**, 1174. (u) A. L. Gott, G. J. Clarkson, R. J. Deeth, M. L. Hammond, C. Morton and P. Scott, *Dalton Trans*., 2008, 2983; (v) D. C. Leitch, P. R. Payne, C. R. Dunbar and L. L. Schafer, *J. Am. Chem. Soc*., 2009, **131**, 18246; (w) J. A. Bexrud and L. L. Schafer, *Dalton Trans*., 2010, **39**, 361; (x) A. L. Reznichenko and K. C. Hultzsch, *Organometallics*, 2010, **29**, 24; (y) L. E. N. Allan, G. J. Clarkson, D. J. Fox, A. L. Gott and P. Scott, *J. Am. Chem. Soc*., 2010, **132**, 15308; (z) K. Manna, S. Xu and A. D. Sadow, *Angew. Chem. Int. Ed*., 2011, **50**, 1865; (aa) D. C. Leitch, R. H. Platel and L. L. Schafer, *J. Am. Chem. Soc*., 2011, **133**, 15453; (ab) K. Manna, W. C. Everett, G. Schoendorff, A. Ellern, T. L. Windu and A. D. Sadow, *J. Am. Chem. Soc*., 2013, **135**, 7235; (ac) E. Chong, S. Qayyum, L. L. Schafer and R. Kempe, *Organometallics,* 2013, **32**, 1858.

5 For cyclohydroamination mediated by group 5 metals, see: (a) A. L. Reznichenko, T. J. Emge, S. Audörsch, E. G. Klauber and K. C. Hultzsch, *Organometallics*, 2011, **30**, 921; (b) F. Zhang, H. Song and G. Zi, *Dalton Trans*., 2011, **40**, 1547.

6 For cyclohydroamination mediated by organoactinides, see: (a) B. D. Stubbert, C. L. Stern and T. J. Marks, *Organometallics*, 2003, **22**, 4836; (b) B. D. Stubbert and T. J. Marks, *J. Am. Chem. Soc*., 2007, **129**, 4253; (c) B. D. Stubbert and T. J. Marks, *J. Am. Chem. Soc*., 2007, **129**, 6149; (d) E. M. Broderick, N. P. Gutzwiller and P. L. Diaconescu, *Organometallics*, 2010, **29**, 3242; (e) C. E. Hayes, R. I. H. Platel, L. L. Schafer and D. B. Leznoff, *Organometallics*, 2012, **31**, 6732.

7 For cyclohydroamination mediated by late transition metals, see: (a) T. E. Müller and A.-K. Pleier, *J. Chem. Soc*., *Dalton Trans*., 1999, 583; (b) T. E. Müller, M. Grosche, E. Herdtweck, A.-K. Pleier, E. Walter and Y.-K. Yan, *Organometallics*, 2000, **19**, 170; (c) T. Kondo, T. Okada, T. Suzuki, and T. Mitsudo, *J. Organomet. Chem*., 2001, **622**, 149; (d) S. Burling, L. D. Field, B. A. Messerle and P. Turner, *Organometallics*, 2004, **23**, 1714; (e) L. M. Lutete, I. Kadota and Y. Yamamoto, *J. Am. Chem. Soc*., 2004, **126**, 1622; (f) L. D. Field, B. A. Messerle, K. Q. Vuong and P. Turner, *Organometallics*, 2005, **24**, 4241; (g) G. B. Bajracharya, Z. Huo and Y. Yamamoto, *J. Org. Chem*., 2005, **70**, 4883; (h) Ch. F. Bender and R. A. Widenhoefer, *J. Am. Chem. Soc*., 2005, **127**, 1070; (i) F. E. Michael and B. M. Cochran, *J. Am. Chem. Soc*., 2006, **128**, 4246; (j) A. Takemiya and J. F. Hartwig, *J. Am. Chem. Soc*., 2006, **128**, 6042; (k) N. T. Patil, L. M. Lutete, H. Wu, N. K. Pahadi, I. D. Gridnev and Y. Yamamoto, *J. Org. Chem*., 2006, **71**, 4270; (l) B. M. Cochran and F. E. Michael, *J. Am. Chem. Soc*., 2008, **130**, 2786; (m) Z. Liu and J. F. Hartwig, *J. Am. Chem. Soc*., 2008, **130**, 1570; (n) E. B. Bauer, G. T. S. Andavan, T. K. Hollis, R. J. Rubio, J. Cho, G. R. Kuchenbeiser, T. R. Helgert, C. S. Letko and F. S. Tham, *Org. Lett*., 2008, **10**, 1175; (o) H. Ohmiya, T. Moriya and M. Sawamura, *Org. Lett*., 2009, **11**, 2145; (p) K. D. Hesp, S. Tobisch and M. Stradiotto, *J. Am. Chem. Soc*., 2010, **132**, 413; (q) L. D. Julian and J. F. Hartwig, *J. Am. Chem. Soc*., 2010, **132**, 13813; (r) Y. Kashiwame, S. Kuwata and T. Ikariya, *Chem. Eur. J*., 2010, **16**, 766; (s) Z. Liu, H. Yamamichi, S. T. Madrahimov and J. F. Hartwig, *J. Am. Chem. Soc*., 2011, **133**, 2772; (t) T. O. Nguyen, Y. W. Man, R. Hodgson and B. A. Messerle, *Aust. J. Chem*., 2011, **64**, 741; (u) Z. G. Specht, S. A. Cortes-Llames, H. N. Tran, C. J. van Niekerk, K. T. Rancudo, J. A. Golen, C. E. Moore, A. L. Rheingold, T. J. Dwyer and D. B. Grotjahn, *Chem. Eur. J*. **2011**, *17*, 6606; (v) Y. Kushiwame, S. Kuwata and T. Ikariya, *Organometallics*, 2012, **31**, 8444; (w) E. Bernoud, P. Oulié, R. Guillot, M. Mellah and J. Hannedouche, *Angew. Chem*., 2014, **126**, 5030, (*Angew. Chem. Int. Ed*., 2014, **53**, 4930).

8 For zinc-catalysed cyclohydroamination, see: (a) A. Zylus, M. Dochnahl, D. Hollmann, K. Löhnwitz, J-St. Hermann, P. W. Roesky and S. Blechert, *Angew. Chem*., 2005, **117**, 7972, (*Angew. Chem. Int. Ed*., 2005, **44**, 7794); (b) M. Dochnahl, J.-W. Pissarek, S. Blechert, K. Löhnwitz and P. W. Roesky, *Chem. Commun*., 2006, 3405; (c) M. Dochnahl, K. Löhnwitz, J.-W. Pissarek, M. Biyikal, S. R. Schulz, S. Schön, N. Meyer, P. W. Roesky and S. Blechert, *Chem. Eur. J*., 2007, **13**, 6654; (d) K. Löhnwitz, M. J. Molski, A. Lühl, P. W. Roesky, M. Dochnahl and S. Blechert, *Eur. J. Inorg. Chem*., 2009, 1369; (e) M. Dochnahl, K. Löhnwitz, A. Lühl, J. W. Pissarek, M. Biyikal, P. W. Roesky and S. Blechert, *Organometallics*, 2010, **29**, 2637; (f) A. Mukherjee, T. K. Sen, P. K. Ghorai and S. K. Mandal, *Organometallics*, 2013, **32**, 7213.

9 For gold-catalysed cyclohydroamination, see: (a) X. Han and R. A. Widenhoefer, *Angew. Chem*., 2006, **118**, 1779, (*Angew. Chem. Int. Ed*., 2006, **45**, 1744); (b) J. Zhang, C.-G. Yang and C. He, *J. Am. Chem. Soc*., 2006, **128**, 1798; (c) Ch. F. Bender and R. A. Widenhoefer, *Chem. Commun*., 2006, 4143; (d) J.-E. Kang, H.-B. Kim, J.-W. Lee and S. Sin, *Org. Lett*., 2006, **8**, 3537; (e) D. Kadzimirsz, D. Hildebrandt, K. Merz and G. Dyker, *Chem. Commun*., 2006, 661; (f) R. L. LaLonde, B. D. Sherry, E. J. Kang and F. D. Toste, *J. Am. Chem. Soc*., 2007, **129**, 2452; (g) R. A. Widenhoefer, *Chem. Eur. J*., 2008, **14**, 5382; (h) C. F. Bender and R. A. Widenhoefer, *Chem. Commun*., 2008, 2741; (i) R. L. LaLonde, Z. J. Wang, M. Mba, A. D. Lackner and F. D. Toste, *Angew. Chem. Int. Ed*., 2010, **49**, 598; (j) Z. J. Wang, D. Benitez, E. Tkatchouk, W. A. Goddard III and F. D. Toste, *J. Am. Chem. Soc*., 2010, **132**, 13064.

10 For cyclohydroamination mediated by alkali metals, see (a) P. Horrillo Martínez, K. C. Hultzsch and F. Hampel, *Chem. Commun*., 2006, 2221; (b) J. Deschamp, J. Collin, J. Hannedouche and E. Schulz, *Eur. J. Org. Chem*., 2011, 3329.

11 For cyclohydroamination mediated by alkaline earth metals, see (a) M. R. Crimmin, I. J. Caseley, and M. S. Hill, *J. Am. Chem. Soc*., 2005, **127**, 2042; (b) S. Datta, P. W. Roesky and S. Blechert, *Organometallics*, 2007, **26**, 4392; (c) F. Buch and S. Harder, *Z. Naturforsch. B*, *J. Chem. Sci*., 2008, **63**, 63169; (d) M. R. Crimmin, M. Arrowsmith, A. G. M. Barrett, I. J. Casely, M. S. Hill and P. A. Procopiou, *J. Am. Chem. Soc*., 2009, **131**, 9670; (e) X. Zhang, T. J. Emge and K. C. Hultzsch, *Organometallics*, 2010, **29**, 5871; (f) J. F. Dunne, D. B. Fulton, A. Ellern and A. D. Sadow, *J. Am. Chem. Soc*., 2010, **132**, 17680; (g) J. Jenter, R. Köppe and P. W. Roesky, *Organometallics*, 2011, **30**, 1404; (h) M. Arrowsmith, M. R. Crimmin, A. G. M. Barrett, M. S. Hill, G. Kociak-Köhn and P. A. Procopiou, *Organometallics*, 2011, **30**, 1493; (i) X. Zhang, T. J. Emge and K. C. Hultzsch, *Angew. Chem*., 2012, **124**, 406, (*Angew. Chem. Int. Ed*., 2012, **51**, 394); (j) X. Zhang, T. J. Emge and K. C. Hultzsch, *Angew. Chem*., 2012, **124**, 406, (*Angew. Chem. Int. Ed*. **2012**, *51*, 394); (k) B. Liu, T. Roisnel, J.-F. Carpentier and Y. Sarazin, *Chem. Eur J*., 2013, **19**, 13445

12 For aluminium-catalysed cyclohydroamination, see: (a) J. Koller and R. G. Bergman, *Chem. Commun*., 2010, **46**, 4577; (b) J. Koller and R. G. Bergman, *Organometallics*, 2010, **29**, 3350; (c) M. Khandelwal, and R. J. Wehmschulte, *J. Organomet. Chem*., 2012, **696**, 4179.

13 X. Cheng, Y. Xia, H. Wei, C. Zhang, Y. Li, G. Qian, X. Zhang, K. Li and W. Li, Eur. J. Org. Chem., 2008, 1929.

14 L. E. N. Allan, D. J. Fox, R. J. Deeth, A. L. Gott and P. Scott, Proceedings of the 42nd IUPAC Congress, Glasgow, 2–7 August 2009.

15 (a) S. Tobisch, *Chem. Eur. J.*, 2011, **17**, 14974; (b) S. Tobisch, *Dalton Trans.*, 2012, **41**, 9182; (c) S. Tobisch, *Inorg. Chem.*, 2012, **51**, 3786.

16 (a) Substrate association and dissociation at the various intermediates is presumably facile and rapid equilibria are expected. (b) Examination by a linear-transit approach gave no indication that such processes are associated with a significant enthalpic barrier. (c) All the attempts to localise species with more than two adducted amine molecules were unsuccessful.

17 (a) The observed $HNMe_2$-adducted phenylene-diamine [(pda)Al(NMe_2)•$NHMe_2$] aluminium amido starting material **2**•A (with the appropriate number of substrate and $HNMe_2$ molecules) has been chosen as reference for relative free energies (kcal mol^{-1}). (b) The prevalent [(pda)Al(NHR)•(NH_2R)] mono-amine adduct $\mathbf{3_1}$'•S, featuring a chelating amidoalkene unit, of the catalytically competent phenylene-diamine aluminium amidoalkene compound (with the appropriate number of substrate (S) or cycloamine (P) molecules) has been chosen as reference for relative free energies (kcal mol^{-1}).

18 The Ar groups of the phenylene-diamine (pda)Al ligand backbone ($(pda)^{2-}$ = $[ArN(C_6H_4)NAr]^{2-}$ with Ar = 3,5-^{t}Bu-C_6H_3) are in grey in order to enhance the visualisation of crucial structural aspects.

19 The prevalent mono-amine adduct $\mathbf{3_1}$'•S of the catalytically (pda)Al amidoalkene compound is the assumed catalyst resting state. However, it is noted that the predicted narrow energy gap between conceivable candidates makes any firm conclusions about the precise nature of the catalyst resting state impossible.

20 Cyclisation of aminoalkene S mediated by (pda)Al amido starting material **2** has been reported (ref. 12a) to reach 72% conversion after 90 h at 423.15 K.

21 R. G. Parr and W. Yang, *Density-Functional Theory of Atoms and Molecules*, Oxford University Press, 1989.

22 (a) R. Ahlrichs, M. Bär, M. Häser, H. Horn and C. Kölmel, *Chem. Phys. Lett.*, 1989, **162**, 165; (b) O. Treutler and R. Ahlrichs, *J. Chem. Phys.*, 1995, **102**, 346; (c) R. Ahlrichs, F. Furche, C. Hättig, W. Klopper, M. Sierka and F. Weigend, *TURBOMOLE*, *version 6.6*; University of Karlsruhe, Karlsruhe, (Germany), 2014; http://www.turbomole.com.

23 (a) P. A. M. Dirac, *Proc. R. Soc. London, Ser. A*, 1929, **123**, 714; (b) J. C. Slater, *Phys. Rev.*, 1951, **81**, 385; (c) S. Vosko, L. Wilk and M. Nusiar, *Can. J. Phys.*, 1980, **58**, 1200; (d) A. D. Becke, *Phys. Rev.*, 1988, **A38**, 3096; (e) J. P. Perdew, *Phys. Rev.*, 1986, **B33**, 8822.

24 (a) O. Vahtras, J. Almlöf and M. W. Feyereisen, *Chem. Phys. Lett.*, 1993, **213**, 514; (b) K. Eichkorn, O. Treutler, H. Öhm, M. Häser and R. Ahlrichs, *Chem. Phys. Lett.*, 1995, **242**, 652.

25 (a) S. Grimme, J. Anthony, S. Ehrlich and H. Krieg, *J. Chem. Phys.*, 2010, **132**, 154104; (b) S. Grimme, S. Ehrlich and L. Goerigk, *J. Comput. Chem.*, 2011, **32**, 1456; (c) http://toc.uni-muenster.de/DFTD3/ getd3.html.

26 (a) F. Weigend and R. Ahlrichs, *Phys. Chem. Chem. Phys.*, 2005, **7**, 3297; (b) F. Weigend, *Phys. Chem. Chem. Phys.*, 2006, **8**, 1057.

27 (a) A. Schäfer, C. Huber and R. Ahlrichs, *J. Chem. Phys.*, 1994, **100**, 5829; (b) K. Eichkorn, F. Weigend, O. Treutler and R. Ahlrichs, *Theor. Chem. Acc.*, 1997, **97**, 119; (c) A. Schäfer, C. Huber and R. Ahlrichs, *J. Chem. Phys.*, 1992, **97**, 2571.

28 S. Grimme, *J. Chem. Phys.*, 2006, 124.

29 P. Plessow, *J. Chem. Theory Comp*. 2013, **9**, 1305.

30 (a) A. Klamt and G. Schüürmann, *J. Chem. Soc. Perkin Trans. 2,* 1993, 799; (b) A. Klamt, *J. Phys. Chem.*, 1995, **99**, 2224; (c) F. Eckert and A. Klamt, *AlChE J.*, 2002, **48**, 369.

31 Y. Okuno, *Chem. Eur. J.*, 1997, **3**, 212.

32 For further details, see http://www.struked.de.

TABLE OF CONTENTS GRAPHIC ENTRY

Aluminium-catalysed intramolecular hydroamination of aminoalkenes: Computational perusal of alternative pathways for aminoalkene activation

Sven Tobisch

Rival mechanistic pathways for C=C bond activation in aluminium-catalysed hydroamination: Computational mechanistic analysis reveals that a catalytically relevant (pda)Al(NHR) compound promotes hydroamination through a stepwise σ-bond insertive mechanism with turnover-limiting aminolysis.